

Electronic Supplementary Information

Confining Al-Li alloy between pre-constructed conductive buffers for advanced aluminum anode

Ning Dong,^{a,b,§} Hao Luo^{a,§}, Yonggao Xia^a, Haocheng Guo^a, Rusheng Fu^a, Zhaoping

Liu^{a, *}

^a Advanced Li-ion Battery Engineering Laboratory and Key Laboratory of Graphene Technologies
and Applications of Zhejiang Province, Ningbo Institute of Materials Technology & Engineering,
Chinese Academy of Sciences, Zhejiang 315201, P. R. China

^b College of Materials Science and Opto-Electronic Technology, University of Chinese Academy of
Sciences, Beijing 100049, P. R. China

* Corresponding author: liuzp@nimte.ac.cn

§ These two authors contributed equally to this work.

Experimental section

- 1. Synthesis of electrode materials.** The sandwich structured anode was prepared *via* a simple physical synthesis. Two pieces of Nickel foams were employed and pressed with one piece of Al foil by 20MPa mechanical pressure for the fabrication of Ni-Al-Ni composite electrode. Before the assembly of coin cells, the Al foil and Ni-Al-Ni composite pole pieces were all treated by 40-minutes short circuit for pre-lithiated process with lithium foil for use. The cathode materials containing 90 wt.% LiFePO₄, 5 wt.% carbon black and 5 wt.% polyvinylidene difluoride (PVDF) were stirred in N-methyl pyrrolidine (NMP) for 10 hours and then coated on Al foil. The sheets were subsequently dried overnight at 80°C and cut into pieces as cathode.
- 2. Electrochemical Measurements.** The electrochemical cycling performance was implemented on the LAND-CT2001A cell testing system (Jinnuo Wuhan Corp., China) with CR2032-type coin cells. The electrolyte was 1M LiPF₆ in ethyl methyl carbonate (EMC) and fluoroethylene carbonate (FEC) (volume ratio 8 : 1). The current density of full cells varied from 0.1C to 2C, and the voltage range was 2.6V-3.8V. Electrochemical impedance spectroscopy (EIS) was performed with the coin cells at room temperature using Solartron 1470E multi-channel battery test system. The impedance spectra were tested with an AC amplitude of 10 mV over a frequency range of 100-0.01 KHz. The impedance data were simulated by the ZSimpWin program.
- 3. Materials characterization.** The scanning electron microscopy (SEM) images of the electrodes were acquired by using a field emission scanning electron microscopy (FESEM, S-4800, Hitachi, Japan). The cycled electrodes were quickly moved into the SEM chamber after washed with DMC for several times in the Ar-filled glove box to minimize the time exposed in the air. Powder X-ray diffraction (XRD) measurements were carried out using an AXS D8 Advance diffractometer from Bruker Inc to identify the crystalline phase of the electrode materials. The data was achieved at 298K with Cu K α radiation at 40 mA and 40 kV in the 2 θ range of 10-80° for cathode and 20-80° for anode with a step size 0.02°. The composition of the SEI layers were characterized by X-ray photoelectron spectroscopy (XPS,

Kratos AXIS Ultra DLD) with Al K α radiation and the curve fitting of the raw data was performed using a peak-fit program.

The description of XPS results: compositional analysis of the SEI layer on the surface of the Al anode and the Ni–Al–Ni anode after cycling was performed by XPS and the results are displayed in Fig. S4. According to the C 1s, O 1s and F 1s spectra, the SEI films are mainly composed of ROLi, ROCOOLi, Li₂CO₃ and LiF, which are generated from the decomposition of the electrolyte. The composition of the SEI layers on the Al anode and the Ni–Al–Ni anode shows little difference due to the fact that the same electrolytes are used for the batteries.

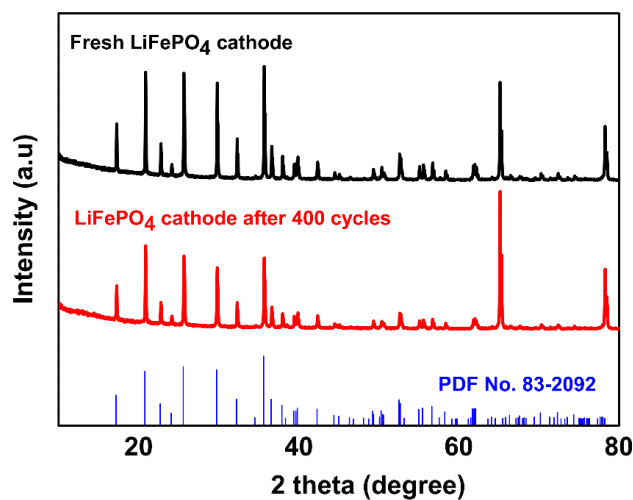


Figure S1. XRD patterns of the LiFePO₄ cathode in the LFP/Ni-Al-Ni battery before and after 400 cycles at 0.2C.

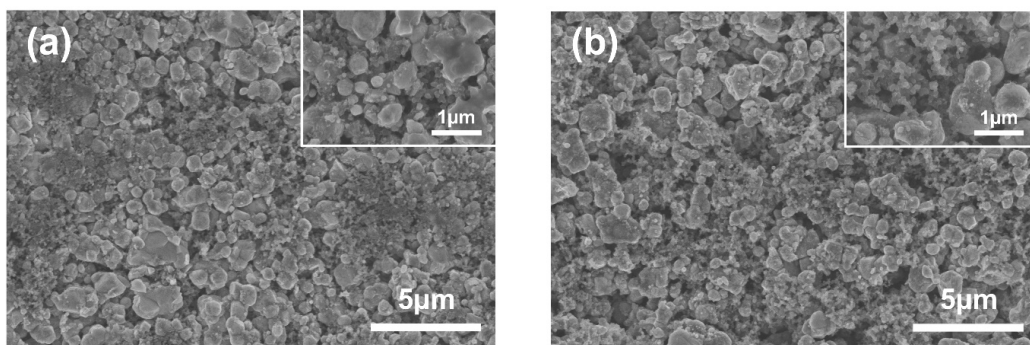


Figure S2. SEM images of the LiFePO_4 cathode in the LFP/Ni-Al-Ni battery (a) before and (b) after 400 cycles at 0.2C. Insets of (a) and (b) are the corresponding enlarged SEM images.

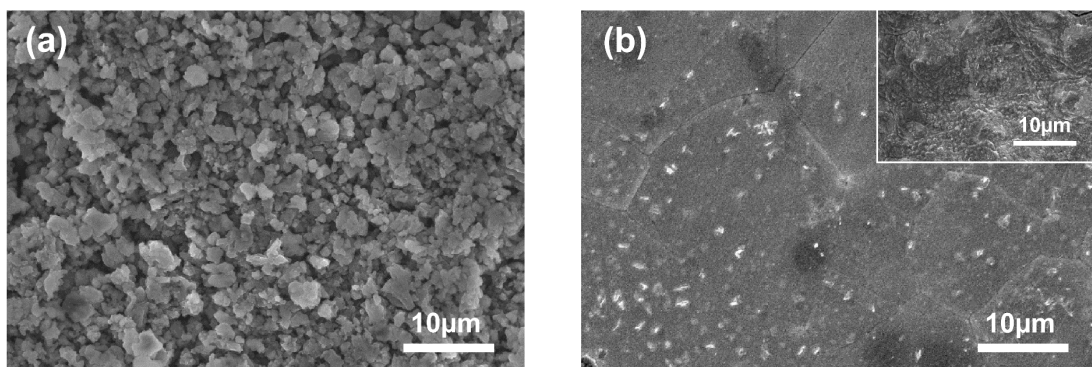


Figure S3. High-resolution SEM images of the surface of (a) Al anode and (b) Ni-Al-Ni anode (nickel foam and Al foil respectively) after cycling.

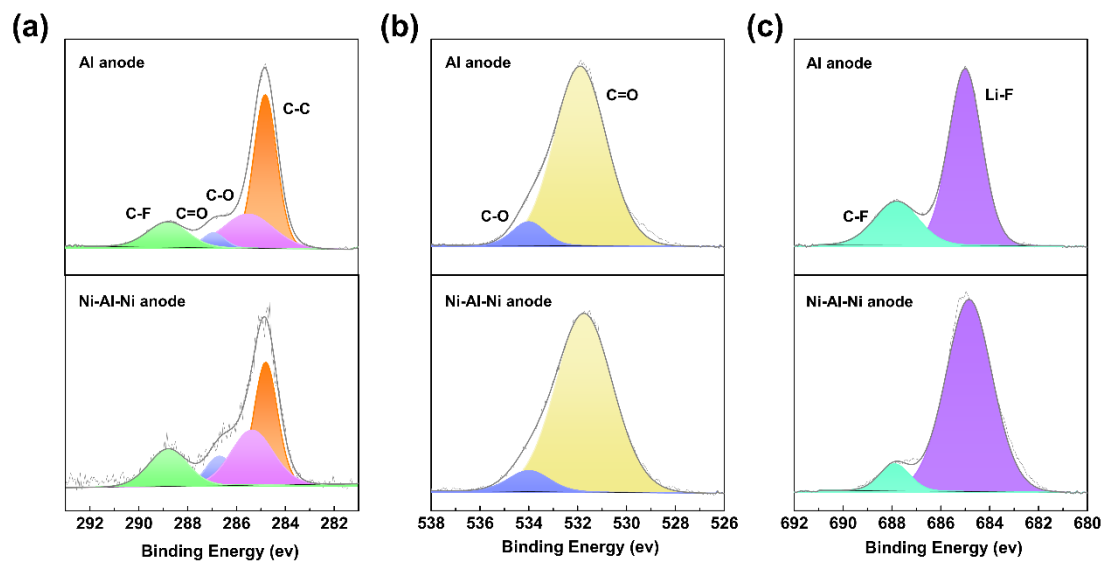


Figure S4. (a) C 1s, (b) O 1s and (c) F 1s X-ray photoelectron spectra of Al anode and Ni-Al-Ni anode after 50 cycles at 0.2C.

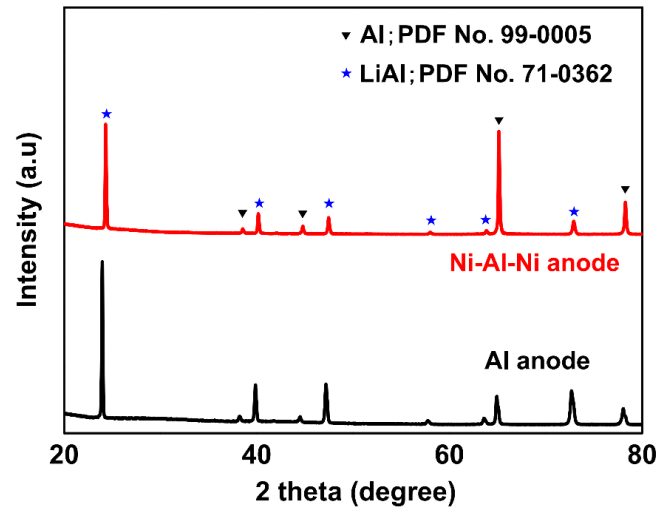


Figure S5. XRD profiles of the Ni-Al-Ni anode and Al anode in a charged battery after 50 cycles.

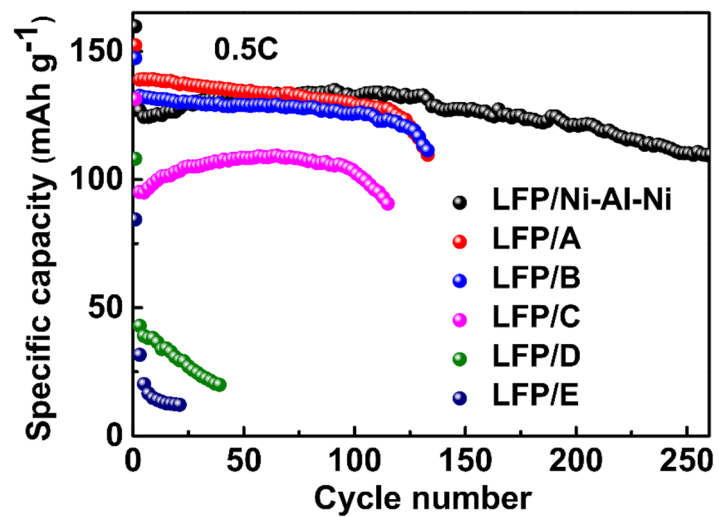


Figure S6. Long-term cycling performance of the full cells with sandwich-structured Ni-Al-Ni anode and five control groups named as A, B, C, D and E at 0.5C.

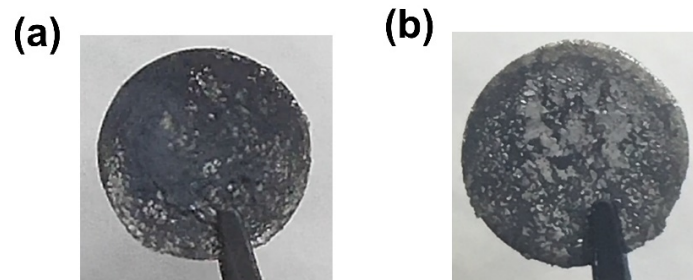


Figure S7. The optical photographs of Ni-Al (control group A) and Al-Ni (control group B) composite anodes after cycling at 0.5C.

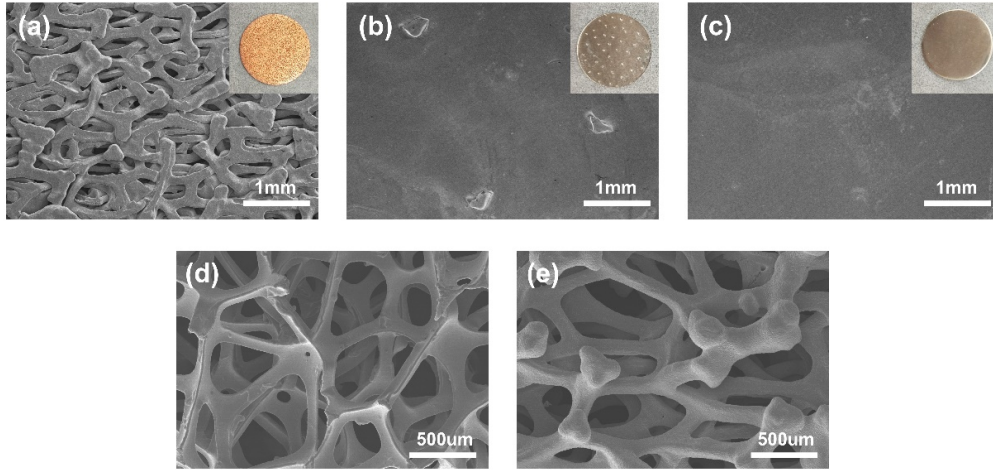


Figure S8. SEM images of (a) control group C, (b) control group D and (c) control group E composite anodes, insets are the corresponding optical photographs. (d, e) SEM images of nickel foam and cu foam respectively.